

Band Rejections for WLAN and WIMAX Utilizing UWB Planar Antenna by Slits in the Conductor Elements

Siti Fatimah Jainal^{1,2*}, Norliza Mohamed³, Azura Hamzah¹

¹Malaysia-Japan International Institute of Technology (MJIIT),
UTM Kuala Lumpur, MALAYSIA

²Faculty of Engineering,
Lincoln University College, Kelana Jaya, Selangor, MALAYSIA

³Razak Faculty of Technology and Informatics,
UTM Kuala Lumpur, MALAYSIA

DOI: <https://doi.org/10.30880/ijie.2020.12.06.002>

Received 8 August 2019; Accepted 28 May 2020; Available online 02 July 2020

Abstract: Band rejections for WLAN and WIMAX frequency bandwidths are realized in a UWB planar antenna utilizing a single slit in an elliptical element. WLAN and WIMAX communication system frequency bandwidths have been known to coexist with the UWB frequency bandwidth. Coexistence of multiple frequency bandwidths are susceptible to disadvantage and could cause interferences to other communication system. The disadvantages could be in form of signal disruption, data loss and equipment malfunctions [1-3]. Thus, it is essential to eliminate WLAN frequency bandwidth from the UWB communication system. Slits are employed to influence the exterior current distribution on the radiator and therefore, has generated mismatched of the input impedance. The phenomenon has caused the band notch characteristic and thus, rejected the frequency bandwidths for 5 to 6 and 3.3 to 3.7GHz, respectively. The structures of the slits are simple in a compact design of the UWB planar antenna. The UWB planar antennas with band rejections are compared with the reference antenna. The reflection coefficients S_{11} for the designed UWB planar antennas have rejected the frequency bandwidths for 5 to 6 and 3.3 to 3.7GHz, consecutively. The peak of the notched-band reflection coefficient S_{11} for the frequency bandwidths 5 to 6 and 3.3 to 3.7GHz are about -3 and -4dB, respectively. Surface currents are distributed in the slit areas. The radiation patterns are illustrated for the frequency 3.5, 7.5 and 9.5GHz for the single notched-band, while 4.5, 7.5 and 9.5GHz for the dual notched-band characteristics. Radiation patterns for the single and dual notched-band in the H- and E-planes for the designed antennas are in omni- and bi-directional, respectively. Maximum gains G are in the $-z$ and $-x$ direction in the H- and E- plane, for the UWB planar antenna with single and dual notched-band characteristics.

Keywords: UWB, WLAN, WIMAX, band notch, slit

1. Introduction

Ultra wideband communication system is allocated between 3.1 and 10.6GHz and has been used to transfer large amount of data wirelessly over a short distance [4]. Furthermore, UWB technology has been used for radar and military applications [5], secure wireless vehicle and tool tracking for aircraft manufacturing, detection of human respiration behind obstacle using impulse uwb radar [6], and localization and tracking of the robot gripper in industrial environment [7]. Variety of UWB applications are led to enhancing of its performances [8-9].

However, UWB frequency bandwidth is coexisted with other communication systems and interference occurrences are unavoidable. For example, it could be destructive for system performance [10] and uwb interference signal as noise in the narrowband radio system [11]. Further signal interferences are discussed in [12-15]. Thus, it is essential to reject the coexisted frequency bandwidths from the UWB communication system accordingly.

Methods such as electromagnetic bandgap, etching in the conductor planes, parasitic elements and ring resonator [16] are utilized in an antenna designs in the means of realizing notched band to reject unwanted frequency bandwidth in uwb communication systems. Etching methods include slit which is etched in the conductor planes by using abstract or alphabetical and are parametrically studied in order to obtain the wanted frequency bandwidth of the band to be rejected.

Structure and the performance of the UWB planar antennas are explained in part 2 and 3, respectively. The UWB planar antenna with band rejection for 5 to 6GHz is described in [17-18]. The designed antenna is extended to generate the band rejection for the frequency bandwidth from 3.3 to 3.7GHz, accordingly. The UWB planar antenna performances are described and summarized results are concluded in part 4, accordingly.

2. Structures of the UWB Planar Antennas

The reference is known as the UWB planar antenna with an elliptical element as in Fig. 1(a-b) and the dimensions are given in Table 1, respectively. The base used FR4, the permittivity, ϵ_r and electric conductivity tangent delta, δ are given as 4.4 and 0.019. Major and minor radiuses are recognized as L_1 and L_2 , respectively. The substrate and conductor planes thickness are identified as h_s and h_c , respectively. Width and length of the ground element are given as L_g and W_g . Feed F is positioned in the radiator. Ground plane used half ground plane for simplicity and compact structure design. The impedance matching is controlled by the eccentricity e as Eq. 1.

$$e = \sqrt{1 - \frac{(L_2)^2}{(L_1)^2}} \tag{1}$$

UWB planar antenna with a single band rejection that is for 5 to 6GHz is demonstrated as Fig. 1(c), while for dual band rejection for the frequency bandwidths 3.3 to 3.7 and 5 to 6GHz is illustrated in Fig. 1(d), accordingly. Single slit is known as S_1 and is scraped in the $+x$ axis of the radiator and the second slit S_2 is etched in the ground plane in the $-x$ axis. Slit configurations and dimensions are illustrated Fig. 2 and Table 2, respectively. Slit S_1 is realized to cause band rejection for the frequency bandwidth between 5 and 6GHz, while slit S_2 is for rejecting the frequency bandwidth between 3.3 and 3.7GHz. Slit S_2 is longer and more slanted compared to slit S_1 . Width w of slit S_2 is bigger than slit S_1 . Slit structures are optimized in the means of obtaining the maximum mismatching until the notched bands have reached the desired frequency bandwidth. Slit positions are placed in horizontal as the surface current is distributed in vertical polarization. Thus, flat slit is considered to disrupt the exterior current in the radiator and realized the mismatched of the reflection coefficient S_{11} . The UWB planar antennas are analyzed using Computer Simulation Technology (CST) software specifically for high frequency simulation in antenna application. The simulation frequency bandwidth is 3 to 11GHz in an open space boundary condition. Convolved Perfect Match Layer (CPML) is employed as to minimize the reflection.

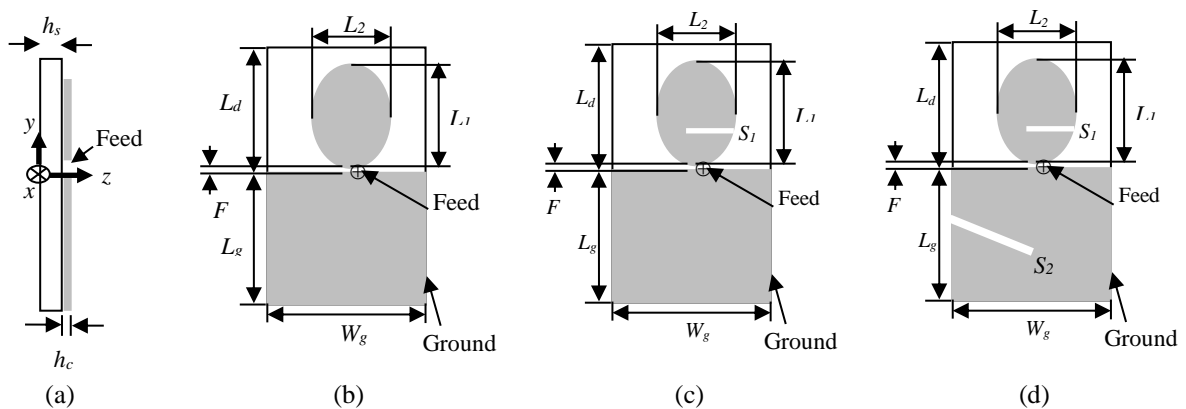


Fig. 1 - (a) side view; (b) reference; (c) UWB planar antenna with a single slit; (d) UWB planar antenna with dual slits

Table 1 - Dimensions of the uwb planar antenna

Parameter	Value (mm)
L_d	21
L_g	24
W_g	21
L_1	16
L_2	12.8
F	0.4
h_s	0.76
h_c	0.035

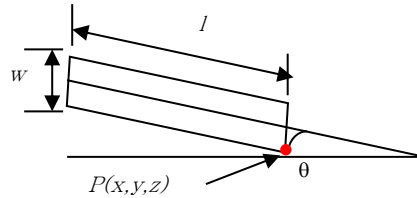


Fig. 2 - Slit configurations for S_1 and S_2

Table 2 - Dimensions of slits

Slit	Parameter	Dimension
S_1	Length, l	8.28 mm
	Width, w	0.13 mm
	Slope angle, θ	1.38 deg
S_2	Length, l	11.27 mm
	Width, w	0.60 mm
	Slope angle, θ	41.04 deg

The reflection coefficient S_{11} for the reference and UWB planar antenna with band rejections are presented in the section 1.2. The notched-band characteristics for the frequency bandwidths 3.3 to 3.7 and 5 to 6GHz are described, accordingly.

2.1 Notched-band Characteristics of the UWB Planar Antennas

UWB planar antenna’s operating frequency bandwidth is accomplished by tuning the eccentricity e . Reflection coefficient S_{11} for eccentricity is illustrated in Fig. 3. Radiator outline is in circular when $e=0$, and a line element for $e=1$. Refer to the finding, UWB operating frequency bandwidth is attained for $e=0$, and $e=0.6$. UWB frequency bandwidth is irrelevant for $e=0.9$ which it does not fulfill the ultra wideband frequency bandwidth. Reflection coefficient S_{11} at $e=0.6$ is overall lesser than $e=0$. Therefore, the radiator dimension when $e=0.6$ is preferred. The finalized reflection coefficient S_{11} of the band rejection for the frequency bandwidth 5 to 6GHz utilizing UWB planar antenna is obtained as in Fig 4. The band rejection is located between 5 and 6GHz and the UWB planar antenna is operated between 3.1 and 10.6GHz which is within the ultra wideband frequency bandwidth. The notched-band peak value for the simulation is about -3.0 and compared with the measured value is about -4.0dB, respectively. Overall, the measured UWB planar antenna with a single band rejection presents lower value of reflection coefficient S_{11} .

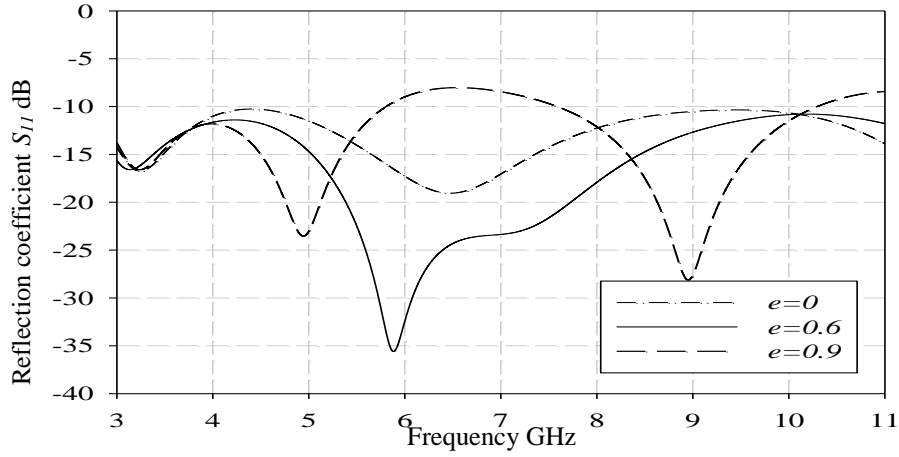


Fig. 3 - Reflection coefficient S_{11} for eccentricity e

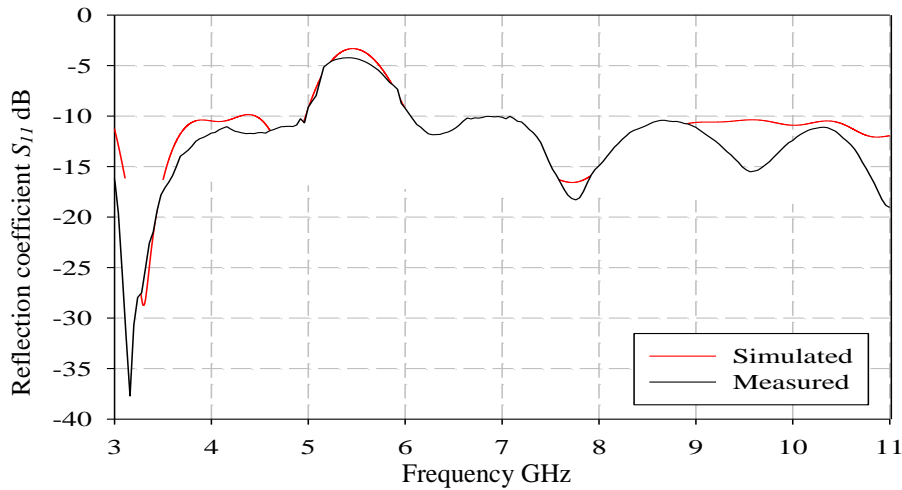


Fig. 4 - Reflection coefficient S_{11} for UWB planar antenna with band rejection for 5 to 6GHz

UWB planar antenna with band rejections for 3.3 to 3.7 and 5 to 6GHz is illustrated in Fig. 5, respectively. The simulated and measured frequency bandwidths for the notched band between 5 and 6GHz are identical. However, the notched-band center frequencies for the measured value are slightly shifted to the lower frequency that is 5.4GHz. The notched-band peaks for the simulated and measured for the frequency bandwidth 5 to 6GHz have reached about -3.0dB. The simulated frequency bandwidth for the second notched band is located between 3.3 and 3.7GHz. However, the measured notched-band frequency bandwidth between 3.2 and 3.7GHz has become slightly wider that is between 3.2 to 3.7GHz, respectively. The notched band between 3.3 and 3.7GHz simulated and measured peak value is about -5.0 and -4.5dB, accordingly. The differences are considered due to the fabrication of the designed UWB planar antennas.

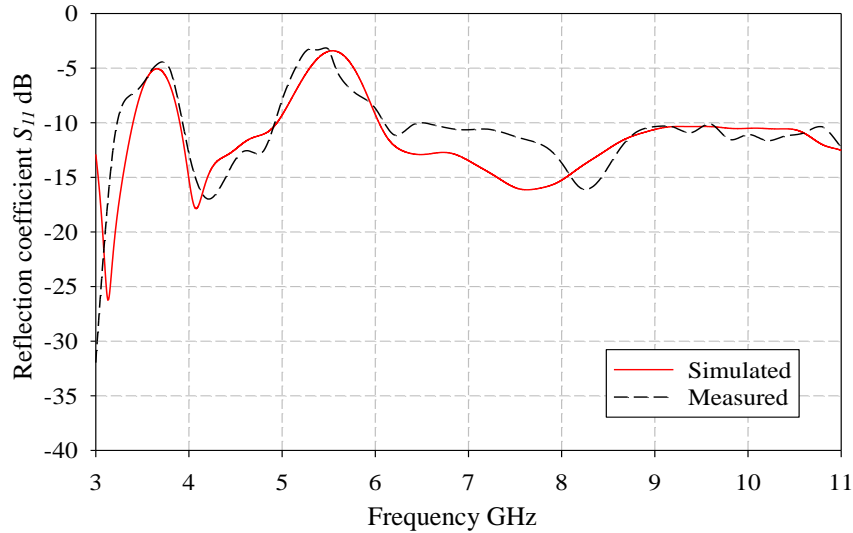


Fig. 5 - Reflection coefficient S_{11} for UWB planar antenna with band rejection for 3.3 to 3.7 and 5 to 6GHz

The notched-band frequency bandwidths for 3.3 to 3.7 and 5 to 6GHz are rejected due to the impedance mismatching in the UWB planar antennas. Slits are considered to interrupt the polarization of exterior current circulation and thus impedance mismatching is realized. The exterior current circulations for the UWB planar antenna with band rejections are presented in the next section. Further exterior current allocations on the conductor surfaces are investigated.

2.2 Surface Current Distribution

The exterior current distributions of the reference and UWB planar antenna comprising slits in the conductor elements are illustrated as in Fig. 6 and 7, consecutively. The exterior current is highly condensed in the radiator and edges of the ground conductor for the reference antenna. The exterior current is distributed vertically from the feed and spread into the conductor element surfaces. The flow of the exterior current is reflected at the edges of the conductor elements. The exterior current polarization is in symmetric for the reference antenna. However, slits existence in the radiator and ground element have resulted the changes in the polarizations of the exterior current distribution on the conductor surfaces. This aspect is considered that affected the radiation patterns of the UWB planar antenna with band rejection. Apparently, the exterior current is distributed in the slits of the radiator and the ground conductor for the band rejection utilizing UWB planar antenna. The exterior current is distributed in the slit in the radiator element for the frequency 5.5GHz, which is at the notched-band center frequency for the UWB planar antenna with band rejection for 5 to 6GHz. Furthermore, the exterior currents are condensed in the slits in the radiator and the ground element at the frequency 5.5 and 3.5GHz for the UWB planar antenna with dual notched band, accordingly. Thus, it is considered that the slits have excited band rejections in the UWB planar antennas.

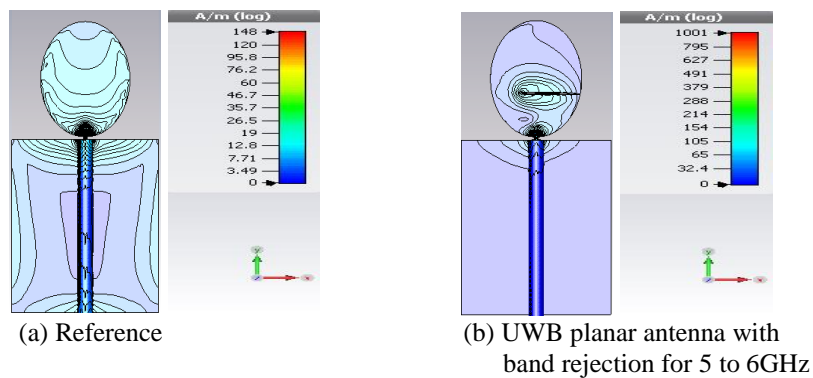


Fig. 6 - Surface current distribution at the frequency 5.5GHz for UWB planar antenna with band rejection for 5 to 6GHz

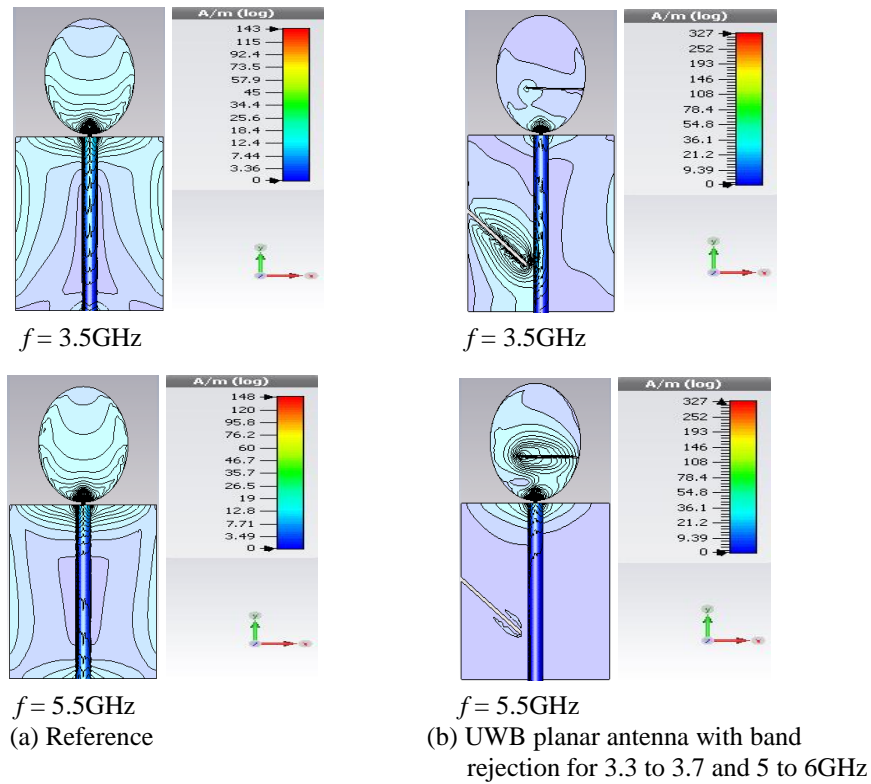


Fig. 7 - Surface current distribution at the frequency 3.5 and 5.5GHz for the UWB planar antenna with band rejection for 3.3 to 3.7 and 5 to 6GHz

2.3 Radiation Pattern

Co-polarization of the radiation patterns for the UWB planar antenna with band rejections are depicted in Fig. 8 and are compared with the reference antenna. Radiation patterns at frequency 3.5, 7.5 and 9.5 GHz are demonstrated for H- and E-plane for the UWB planar antenna with band rejection for 5 to 6GHz in Fig. 8(a). However, the radiation patterns are considered at the frequency 4.5, 7.5 and 9.5GHz, for the UWB planar antenna with band rejections for 3.3 to 3.7GHz and 5 to 6GHz. In both cases, the co-polarizations are in omni-directional for the H-, and E-plane is in bi-directional, respectively. Consequently, the radiation pattern is comparable as monopole antenna.

Maximum gain G_{max} at the frequency 3.5, 7.5 and 9.5GHz is situated in the E-plane for the reference antenna. In addition, the maximum gains in the H-plane for the UWB planar antenna with band rejections are situated in the $-z$ coordinate and E-plane at $-x$ coordinate. Furthermore, the radiation patterns are not significantly exaggerated by the slit in the radiator. Number of lobes increases in the higher frequency region. The simulated and measured radiation patterns for the reference and UWB planar antenna with band rejections are verified. Radiation patterns for the UWB planar antenna with band rejection for 3.3 to 3.7 and 5 to 6GHz at the frequency 7.5GHz is in unsymmetrical. It is considered that the radiation patterns are affected by the slit S_2 in the ground element. It is compared with the radiation patterns for the UWB planar antenna with band rejection for 5 to 6GHz, where the radiation patterns are in symmetric at the frequency 7.5GHz. The maximum gain G over frequency for the UWB planar antenna with band rejections are compared with the reference antenna and it is described in the next section.

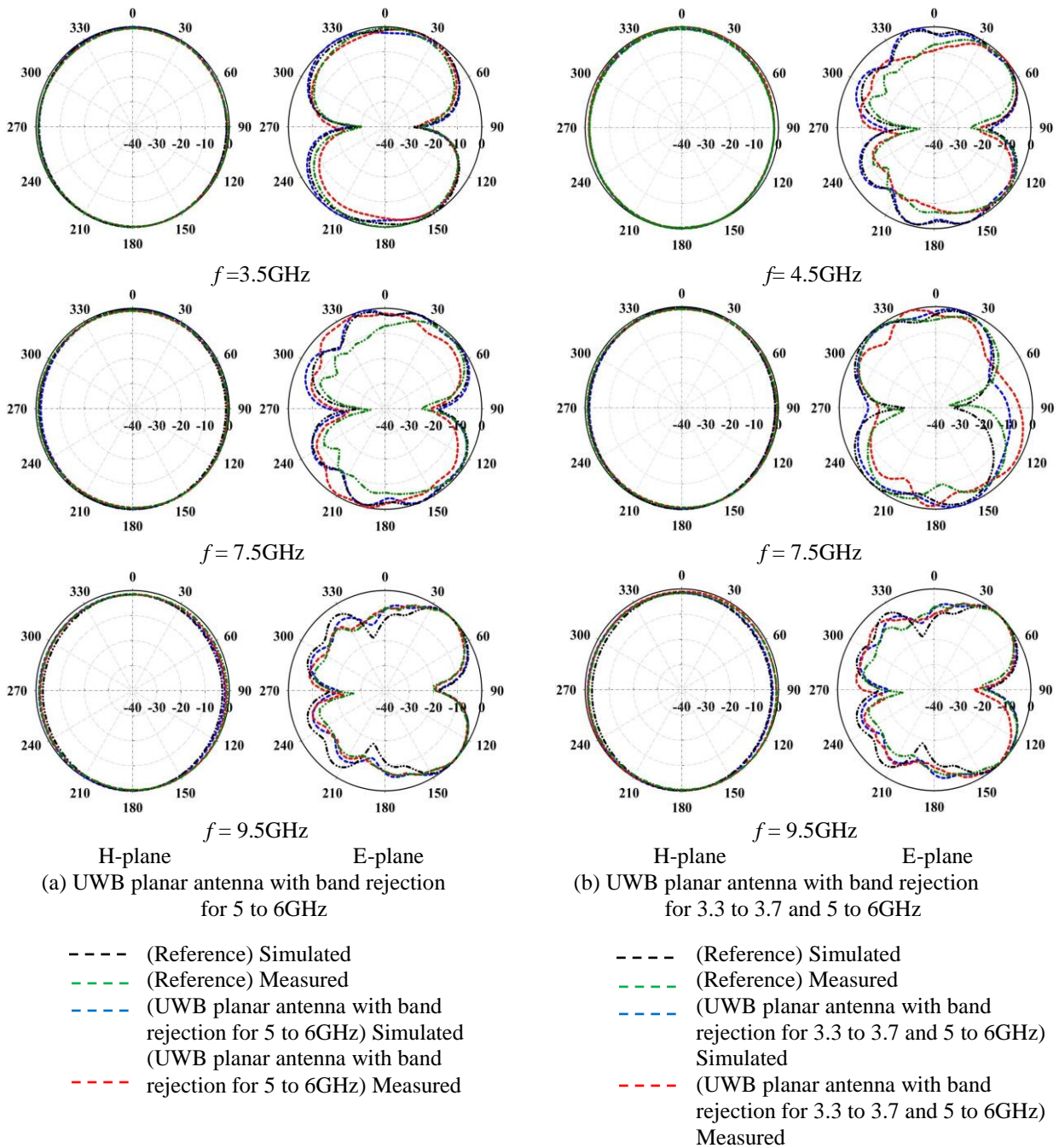


Fig. 8 - Radiation patterns for UWB planar antennas

2.4 Gain G

The antennas maximum gain G versus frequency f is depicted in Fig. 9. Band rejection utilizing UWB planar antenna maximum gain G versus frequency f is generally superior to the reference antenna. Maximum gain G of the reference is given at the frequency 6.4GHz and the band rejection utilizing UWB planar antenna at 6.6GHz, of which $G_{max}=5\text{ dB}$, and $G_{max}=5.4\text{dB}$, respectively. Nonetheless, the maximum gain G has plunged notably at the band rejection frequency bandwidth due to the impedance mismatching. The gain for the UWB planar antenna with band rejection for 5 to 6GHz has reached 2.8dB at the frequency 5.5GHz. Furthermore, the gain at the frequency 3.5 and 5.5GHz have reached 3.6 and 3.7dB for the UWB planar antenna with band rejection for 3.3 to 3.7 and 5 to 6GHz, accordingly. It is considered that in overall, the slits in the conductor elements have not significantly affected the maximum gain over the frequency of the UWB planar antenna with band rejections.

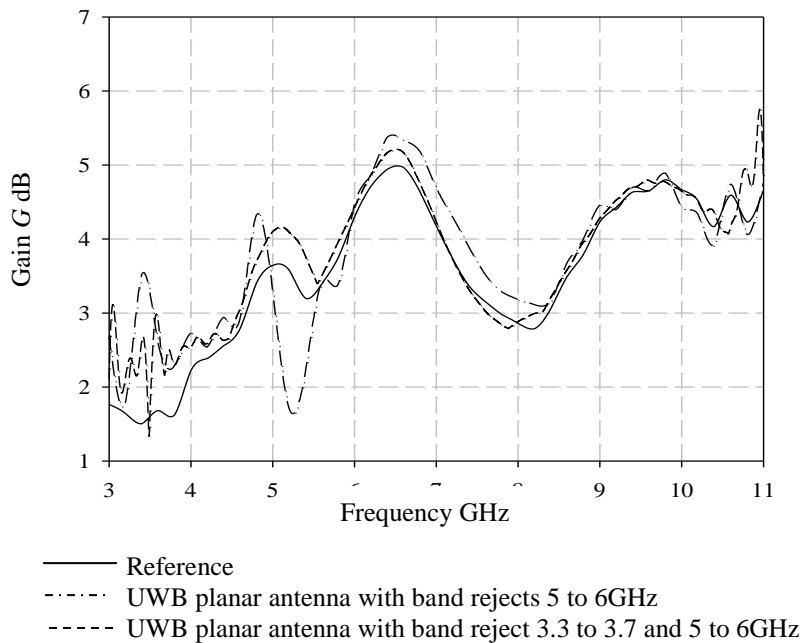


Fig. 9 - Maximum gain G over frequency for UWB planar antennas

3. Conclusion

Band rejection utilizing UWB planar antenna with is investigated and has revealed an improved maximum gain G match up to the reference. Generally, performance of the radiation patterns between reference and the band rejection utilizing UWB planar antenna are considerably unchanged. UWB planar antenna conductor elements consists slits, which are considered to generate band rejections characteristics. The reference and UWB planar antenna with band rejections are compared in term of reflection coefficient S_{11} , radiation pattern and gain. The exterior current allocations are studied and presented.

Acknowledgement

The project is funded by Universiti Teknologi Malaysia (UTM) under Grant No. 4J283.

References

- [1] Taha, A. and Chugg, K.M. (2002). A theoretical study on the effects of interference uwb multiple access impulse radio, Conference Record of the Thirty-Sixth Asilomar Conference on Signals, Systems and Computers. California, USA, paper #7798194
- [2] Swami, A., Sadler, B. and Turner, J. (2001). On the coexistence of ultra-wideband and narrowband radio systems. Proceedings of Communications for Network-Centric Operations: Creating the Information Force (MILCOM). McLean, USA, paper #7354959
- [3] Giorgetti, A., Chiani, M. and Win, M.Z. (2005). The effect of narrowband interference on wideband wireless communication systems. IEEE Transactions on Communications, 53, 2139-2149. Iglesias, E.R., Catherwood, P.A. and William G. Scanlon. (2015). Ultra wideband communications-an idea whose time has still yet to come?. IEEE Antennas and Propagation Magazine, 57, 38-43
- [4] Kumar, V., Samir, G., Pandya, R. and D. Makavana. (2015). Ultra wideband (uwb) communication & its applications. 8th National Level Science Symposium, Rajkot, India, 34-38
- [5] Pavol, G., Alena, G., Stanislav, S., Martin, P., Milos, D., Marek, S. and Ihab, B.A.S. (2018). Robot vision ultra-wideband wireless sensor in non-cooperative industrial environments. International Journal of Advanced Robotic Systems, 1, 1-12
- [6] Mohamed, A., Bahig, H.M. and Hassan, A.M. (2017). Recent approaches to enhance the efficiency of ultra-wide band mac protocols. International Journal of Advanced Computer Science and Applications (IJACSA), 8, 404-410
- [7] Yu, Y., Bing, Z.W. and Shuai, D. (2017). Performance comparison with different antenna properties in time reversal ultra-wideband communications for sensor system applications. Sensors, 18, 1-15

- [8] Farshad, S. and Chahe, N. (2015). Impact of th-uw b interference on mb-ofdm uw b systems: interference modeling and performance analysis. *Wireless Communications and Mobile Computing*, John Wiley & Sons, 16, 960-976
- [9] Gustavo, N. and Annamalai, A. (2007). Ultra wideband (uw b) interference on umts receivers. 2nd International Symposium on Wireless Pervasive Computing (ISWPC), San Juan, Puerto Rico, 105-108
- [10] Nabi, M.A., Jayalakshmi, R. and Umopathy, D.K. (2016). Intentional electromagnetic interferences in communication devices. *International Journal of Scientific & Technology Research (IJSTR)*, 5, 179-183
- [11] Kamran, A. and Valerijs, Z. (2015). Technology implications uw b on wireless sensor network-a detailed survey. *International Journal of Communication Networks and Information Security (IJCNIS)*, 7, 147-161
- [12] Ahmed, B.T. and Miguel, C.R. (2012). *UWB coexistence with 3g and 4g cellular systems*. London: IntechOpen Limited
- [13] Abdulrahman, A., AbdulMalik, A.S., Mansour, A., Ahmad, A., Suheer, A.H., Mai, A.A., and Hend, S.A.K. (2016). Ultra wideband indoor positioning technologies analysis and recent advances. *Sensors*, 16, 1-36
- [14] Moghadasi, M.N., Sadeghzadeh, R.A., Sedghi, T., Aribi, T. and B.S. Virdee, B.S. (2013). Uwb cpw-fed fractal patch antenna with band-notched function employing folded t-shaped element. *IEEE Antennas and Wireless Propagation Letter*, 12, 504-507
- [15] Zhu, F., Gao, S., Ho, A.T.S., Abd-Alhameed, R.A., See, C.H., Brown, T.W.C., Li, J., Wer, G. and J. Xu, J. (2013). Multiple band-notched uw b antenna with band-rejected elements integrated in the feed line. *IEEE Transaction on Antennas and Propagation*, 61, 3952-3960
- [16] Ojaroudi, M. and Ojaroudi, N. (2014). Ultra-wideband small rectangular slot antenna with variable band-stop function. *IEEE Transaction Antennas and Propagation*, 62, 490-494
- [17] Jainal, S.F., Mohamed, N. and Hamzah, A. (2019) Band rejection for wlan utilizing ultra wideband planar antenna. *IEEE Malaysia-Japan Workshop on Radio Technology*, Kuala Lumpur, Malaysia, 1-4
- [18] Jainal, S.F., Wakabayashi, T., Ayob, O. and Rahim, M.K.A. (2013) An uw b planar antenna comprising a single slot elliptical element with band notch characteristics. *IEEE International Conference on RF and Microwave*, Penang, Malaysia, 121-125